THE ASTROPHYSICAL JOURNAL, 208: 336–345, 1976 September 1

THE IONIZATION STRUCTURE OF H II REGIONS: THE EFFECTS OF STELLAR METAL OPACITY*

BRUCE BALICK
Lick Observatory, Board of Studies in Astronomy and Astrophysics, University of California, Santa Cruz
AND
CHRISTOPHER SNEDEN
Department of Physics and Astronomy, University of Wyoming
Received 1975 December 15; revised 1976 January 29

ABSTRACT

Stellar metal opacities in early-type stars are investigated and found to affect the predicted ionization structure of H II regions. Metal absorption edges can drastically diminish the flux of the energetic photons capable of producing the high-ionization species N^{++}, O^{++}, S^{+3}, and Ne^{++} relative to metal-free atmospheres. Moreover, the common assumption that the ionization zones of He^{+} and the high-ionization species are coincident is found to be erroneous. Structural parameters and observable quantities of H II regions are tabulated for ranges of stellar temperatures T_* between 33,000 and 50,000 K, nebular densities of 10 to 1000 cm^{-3}, and metal contents Z between $-0.5 \leq \log(Z/Z_\odot) \leq 1$. An improved variation of the standard metal-abundance determination scheme of Peimbert and Torres-Peimbert is developed. Gradients of Z found in external galaxies by observations of H II regions are briefly discussed, and it is found that a gradient of T_* with galactocentric distance in the presence of a negative Z gradient is not required in order to explain the observations.

Subject headings: nebulae: general — stars: abundances

I. INTRODUCTION

Photoionized nebulae have been the subject of considerable astrophysical interest for many years because the physical processes which govern their rather easily studied emission spectra are fairly well understood. Such nebulae are not only interesting to study in themselves, but have been useful as testing grounds for new physical theories, as delineators of galactic structure and kinematics, and as metersticks for measuring the distance to faint galaxies, to name just a few applications. Of particular recent interest has been the use of H II regions for probing chemical abundances (Peimbert and Costero 1969; Peimbert and Torres-Peimbert 1971, hereafter PTP; Osterbrock 1970, 1974; Rubin 1969, hereafter RHR; Boeshaar 1975) and chemical distribution and evolution in galaxies (Smith 1975*a*; Shields 1974; Shields and Tinsley 1975; Peimbert 1975; Searle 1971).

Optical and infrared emission lines from a rich variety of ionized species of the "metals" (atomic number >2; primarily N, O, Ne, and S) can be observed in H II regions. Because of the manner in which these lines are excited, the observed line intensities and ratios are sensitive to nebular temperatures, densities, and metal abundances. For some applications (e.g., the measurement of chemical abundances), it is important that one or more of the ionic species abundances of metal Z relative to hydrogen $n(Z^{+p})/n(H^{+})$, be determined. These ionic species abundances depend both on the production and destruction rates of the species by photoionization from stellar photons and by recombination with free electrons. Therefore, details of the emergent flux spectrum of stellar photons at frequencies above about 13 eV and the transfer of these photons through the nebula must be known before the ionization structure of the nebula can be properly understood.

The spectrum of stellar ionizing photons cannot be directly measured, and instead must be theoretically calculated. Models of early-star atmospheres are now improving rapidly as better computing techniques develop. Early model calculations indicated that all significant variations of the spectrum of stellar ionizing photons resulted from the bound-free opacity edges of hydrogen and helium. At energies between the ionization potentials of H^0, He^0, and He^+ (13.6, 24.6, and 54.4 eV, respectively) the flux of stellar photons was not thought to exhibit large changes. However, recent model-atmosphere calculations (cf. Hummer and Mihalas 1970*a*, *b*) have shown that metals in the stellar atmosphere can have a large bound-free opacity contribution as well. Therefore, a large fraction of the stellar flux capable of producing some of the metal ionization species in the nebula can be absorbed instead in the stellar atmosphere.

The effects of atmospheric "ionization edge" opacities of metals on the ionization and thermal structure of H II regions have never been properly evaluated. Self-consistent calculations of the stellar atmosphere and the nebula are required wherein the

* *Lick Observatory Bulletin*, No. 727.

various effects of metals as well as of hydrogen and helium are taken into account in both the star and nebula. It is the purpose of this paper to report the results of such calculations and to explore the ramifications of these results on other studies which might be affected. In particular, the procedure for the determination of metal abundances from observations of their optical and infrared lines is critically reviewed. Furthermore, we investigate the question of metal-abundance gradients observed in H II regions of late-type galaxies in the light of the present results.

For the sake of brevity in the discussion which follows, we shall assume some basic familiarity by the reader with the principles of ionization and thermal equilibrium and the methods of abundance determinations. References and summaries of these topics can be found in the references cited above and in Terzian and Balick (1974).

II. ASSUMPTIONS MADE IN DETERMINING METAL ABUNDANCES

Abundances are generally determined by the method reviewed by PTP (with some variations). Briefly, in this procedure the basic structural parameters T_e and n_e, the electron temperature and density, and if possible their rms fluctuations, are determined by ratios of forbidden lines of certain ionization species such as N^+, O^+, O^{++}, and S^+. The results are then combined with ratios of line intensities relative to hydrogen lines, and the ionic species abundances $n(Z^{+p})/n(H^+)$ are calculated relative to ionized hydrogen. The species abundances are then converted into metal abundances, $n(Z)/n(H)$, by making certain assumptions about the nebular ionization structure. Specifically, it is assumed that the H II region can be divided into two distinct ionization zones consisting entirely of H^+ and either the "low-ionization" species He^0, N^+, O^+, Ne^+, and S^+ (or S^{++}) on the one hand, or the "high-ionization" species He^+, N^{++}, O^{++}, Ne^{++}, and S^{+3} on the other (in planetary nebulae a third zone consisting of He^{++} and other higher ionization species is generally required).

The assumption of exclusive nebular ionization zones is predicated on the similarities of the photoionization cross sections and ionization potentials (between 24 and 41 eV) of each of the low-ionization metal species as well as the assumption that the local nebular flux of ionizing radiation is sufficient (or insufficient) to sustain all of the constituent metals in their respective high ionization states. Justification for the latter assumption was based on the older stellar atmosphere calculations; however, more recent calculations of early-type stellar atmospheres, for example by Casinelli (1971) and Hummer and Mihalas (1970*a*, *b*) indicate that many of the more energetic photons

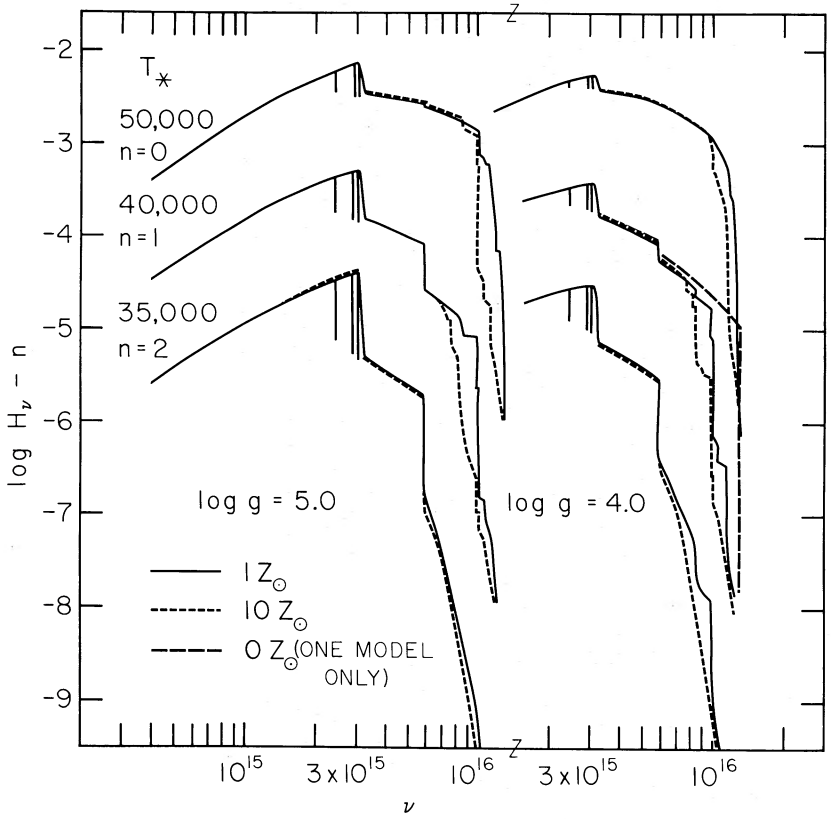

FIG. 1.—Stellar fluxes emergent from early-type stars of temperatures $T_* = 35{,}000$, 40,000, and 50,000 K, $\log g = 4$ and 5, and metal contents $Z = Z_\odot$ and $10\,Z_\odot$ as computed by the ATLAS program (Kurucz 1970).

which produce the high-ionization species in the nebula are absorbed instead by low-ionization species of these metals found in the stellar atmosphere. The emergent spectrum of ionizing radiation is substantially modified by the opacity of these metals, especially at energies above about 35 eV.

III. MODEL CALCULATIONS

a) Stellar Atmospheres

In order to illustrate the effects of the stellar metal opacities, we have computed a series of model atmospheres and nebulae. The atmospheres were calculated for all combinations of effective stellar temperatures $T_* = 35{,}000$, 40,000, and 50,000 K, $\log g = 4$ and 5, and $Z/Z_\odot = 1$ and 10, and are shown in Figure 1. Additional models for which $T_* = 33{,}000$, 37,500, 42,500, and 45,000 K, $\log g = 4$, and $Z/Z_\odot = 1$ were also computed. Here we have adopted the usual notation that Z represents the metal abundances of C, N, O, Ne, and S, and $Z_\odot$ is taken to be (3.2, 0.76, 5.25, 3.2, 0.15) $\times 10^{-4}$, respectively, relative to hydrogen. The helium abundance is assumed to be 10 percent of hydrogen throughout these calculations.

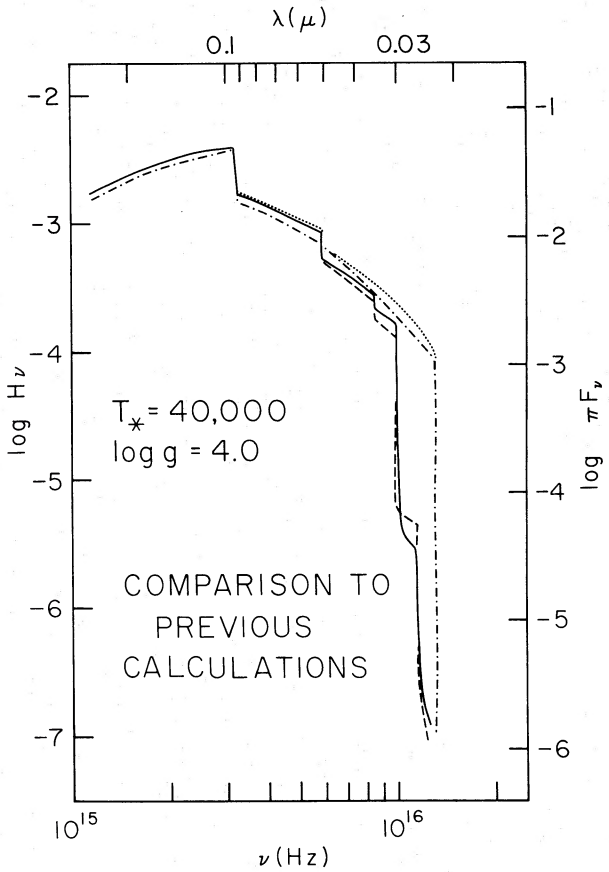

FIG. 2.—Comparison of ATLAS fluxes to previous calculations. The various models are ATLAS ($Z = Z_\odot$, LTE, *solid line*; $Z = 0$, LTE, *dotted line*), Auer and Mihalas 1972 ($Z = 0$, non-LTE, *dot-dashed line*), and Hummer and Mihalas 1970*a*, *b* ($Z \approx Z_\odot$, LTE, *dashed line*). All models are computed for $T_* = 40{,}000$ and $\log g = 4$ assuming plane-parallel geometry.

The models were all calculated using the ATLAS program for model atmospheres (Kurucz 1970). ATLAS was used primarily because of its simplicity of application under a wide variety of conditions. Included are the opacities of the hydrogen lines, H^-, He^-, Rayleigh scattering of H and He, electron scattering, bound-free transitions of H, He, and He^+, and the metal "edges" (i.e., bound-free transitions of C II–IV, N II–V, O II–VI, and Ne I–VI). Plane-parallel geometry and radiative and local thermodynamic (LTE) equilibrium were assumed, but line blanketing from the metal lines was not included.

In Figure 2 we compare the present model emergent flux spectra with two previously published models. The far-ultraviolet fluxes computed by ATLAS for $T_* = 40{,}000$, $Z = 0$, and $\log g = 4$ agree well with a comparable calculation by Auer and Mihalas (1972), who did not assume LTE conditions. Also shown is an ATLAS model for $Z = Z_\odot$ and a model for which $Z \approx Z_\odot$ from Hummer and Mihalas (1970*a*, *b*). For our purposes the differences between comparable models are not important. We should note that the ATLAS models differ appreciably from models with spherical geometry (e.g., Casinelli 1971; Casinelli and Hartmann 1975). The question of the most realistic geometry is undecided at the present time.

In Figures 1 and 2 the absorption "edges" of H^0 and He^0 are conspicuous at 13.6 and 24.6 eV, respectively. Also of considerable importance insofar as the nebular ionization structure is concerned are the effects of the metal opacities. The absorption edges of O^+, Ne^+, and N^{++} combine to strongly modify the stellar fluxes at energies above 35–40 eV, depending on Z, $\log g$, and T_*. Clearly, the flux of photons capable of ionizing these same species in the nebula is substantially diminished relative to the metal-free case.

b) Model Nebulae

We now present the results of the model nebula calculations in which the stellar atmospheres discussed in the previous sections are used. The nebular models were computed using a numerical program (Balick 1975) similar to the programs used by Hjellming (1966) and RHR. The opacities of nebular hydrogen and helium to the ionizing radiation are computed radially from the stellar surface at each of 20 frequencies between 13.6 and 54.4 eV. At each radial point the ionization equilibrium equations for all ionized species and the thermal balance equation are solved in order to compute the local fractional species ionizations $n(R^{+p})/n(R)$ and the electron temperatures. In the process the permitted- and forbidden-line intensities are calculated using a five-level scheme for the latter. Atomic constants are taken from the compilation by Osterbrock (1974), except for newer values given by Seaton (1975). The collisional cross sections used are those appropriate to 10,000 K; variations of the cross sections with temperature are ignored. Charge-exchange processes are not included.

TABLE 1

GLOBAL NEBULAR PARAMETERS ($Z = Z_\odot$)

T_*(K) 33,000	35,000	37,500	40,000	42,500	45,000	50,000	N(H) (cm^{-3})	T_*(K) 33,000	35,000	37,500	40,000	42,500	45,000	50,000
			$x(N^+)$								[NII]λ6583/Hβ*			
0.92	0.77	0.23	0.080	0.053	0.041	0.032	10	110	96	37	15.2	12.3	10.0	8.6
.91	.74	.16	0.043	.029	.022	.017	100	110	93	27	9.1	7.1	5.9	5.0
.87	.71	.10	.022	.016	.012	.009	1000	110	96	19	5.5	4.4	3.6	2.8
			$x(O^+)$								[OII]λλ3727/Hβ*			
0.96	0.89	0.44	0.188	0.117	0.089	0.050	10	220	230	150	99	80	70	46
.95	.86	.31	.105	.063	.046	.026	100	230	220	110	62	48	39	26
.93	.82	.21	.054	.033	.025	.013	1000	230	220	85	34	27	22	14
			$x(O^{++})$								[OIII]λ5007/Hβ*			
0.011	0.083	0.54	0.81	0.88	0.91	0.95	10	2.0	16	140	320	420	490	570
.018	.127	.68	.89	.94	.95	.97	100	3.5	23	180	380	470	530	610
.034	.176	.79	.95	.97	.98	.99	1000	7.9	41	280	490	580	640	720
			$x(Ne^+)$								log [NeII]λ12.8μ†			
0.95	0.97	0.98	0.96	0.79	0.75	0.213	10	-7.43	-7.09	-6.77	-6.40	-6.20	-6.00	-6.17
.97	.98	.98	.93	.66	.60	.119	100	-7.42	-7.08	-6.77	-6.41	-6.23	-6.10	-6.42
.98	.99	.98	.87	.50	.44	.064	1000	-7.42	-7.08	-6.76	-6.44	-6.39	-6.22	-6.69
			$x(Ne^{++})$								[NeIII]λ3869/Hβ*			
0.000	0.001	0.004	0.034	0.21	0.25	0.79	10	<0.1	<0.1	0.1	1.3	11	16	74
.000	.001	.007	.066	.34	.40	.88	100	<0.1	<0.1	0.2	2.8	21	29	90
.000	.001	.016	.127	.50	.56	.94	1000	<0.1	<0.1	0.6	7.4	41	53	120
			$x(S^+)$								[SII]λλ6717+6731/Hβ*			
0.51	0.40	0.246	0.106	0.066	0.050	0.033	10	84	70	51	29	22.9	18.5	14.0
.37	.27	.153	.049	.030	.021	.014	100	62	48	34	16	11.8	9.1	6.7
.26	.17	.089	.019	.016	.010	.007	1000	54	32	21	7	6.5	2.5	3.1
			$x(S^{++})$								[SIII]λ9532/Hβ*			
0.47	0.56	0.52	0.41	0.32	0.262	0.170	10	19	23	22	22	19	17.0	12.0
.62	.68	.48	.30	.20	.159	.097	100	26	29	22	17	13	10.8	7.2
.71	.75	.40	.18	.12	.093	.053	1000	32	35	21	12	9	7.0	4.3
			$x(S^{3+})$								log [SIV]λ10.5μ†			
0.003	0.024	0.22	0.47	0.61	0.69	0.79	10	-10.33	-9.01	-7.71	-7.00	-6.60	-6.32	-5.90
.005	.045	.36	.65	.76	.82	.88	100	-10.03	-8.73	-7.50	-6.86	-6.50	-6.25	-5.85
.010	.077	.51	.80	.86	.89	.92	1000	-9.74	-8.50	-7.33	-6.77	-6.44	-6.20	-5.83
			$x(He^+)$								radio flux (Jy)†			
0.14	0.34	0.93	1.0	1.0	1.0	1.0	10	41	90	200	470	910	1500	3500
.14	.35	.95	1.0	1.0	1.0	1.0	100	41	91	200	480	920	1600	3600
.16	.35	.97	1.0	1.0	1.0	1.0	1000	40	93	210	490	950	1600	3700
			$\langle T_e \rangle_{H^+}$								log (Hβ)†			
7190	7270	7170	7690	8090	8380	8660	10	-7.64	-7.30	-6.99	-6.61	-6.32	-6.09	-5.72
7280	7300	7170	7860	8250	8510	8820	100	-7.63	-7.29	-6.99	-6.60	-6.31	-6.08	-5.71
7450	7570	7700	8370	8720	9010	9290	1000	-7.64	-7.28	-6.96	-6.59	-6.30	-6.07	-5.70
			$\langle T_e \rangle_{O^{++}}$								log [OIII]λ5007/λ4363			
6510	6450	6810	7610	8060	8360	8680	10	2.96	2.95	2.73	2.48	2.39	2.34	2.30
6500	6380	6900	7810	8240	8510	8840	100	2.94	2.95	2.69	2.42	2.34	2.30	2.25
6860	6800	7510	8350	8730	9010	9310	1000	2.80	2.81	2.53	2.32	2.24	2.20	2.15
			$\langle T_e \rangle_{N^+}$								log [NII]λ6583/λ5575			
7270	7470	8010	8700	9210	9620	9880	10	2.17	2.14	2.02	1.90	1.85	1.80	1.78
7360	7570	8250	8950	9590	9790	10000	100	2.15	2.12	1.99	1.86	1.80	1.77	1.76
7590	7840	8760	9410	10300	10400	10700	1000	2.09	2.05	1.91	1.82	1.72	1.71	1.69
			$R_*^\S/R_\odot$								$\Phi(\lambda<912)\ x10^{-48}$‡			
7.9	8.0	8.7	10.2	11.7	12.9	15.1	--	1.1	2.3	5.3	12	22	37	86

*percent †erg $cm^{-2}s^{-1}$ at 500 pc §stellar radius ‡flux of stellar ionizing photons (photons s^{-1})

TABLE 2A

GLOBAL STRUCTURAL PARAMETERS

T_*(K)	35,000				40,000				50,000			
log $(Z/Z_\odot)$	-0.5	0-0	0.5	1.0	-0.5	0.0	0.5	1.0	-0.5	0.0	0.5	1.0
N(H)(cm^{-3})						$x(N^+)$						
10	0.73	0.77	0.83	0.88	0.070	0.080	0.088	0.110	0.020	0.032	0.034	0.042
100	.68	.74	.82	.86	.038	.043	.049	.061	.009	.017	.019	.023
1000	.66	.71	.78	.83	.021	.022	.026	.029	.004	.009	.011	.012
						$x(O^+)$						
10	0.83	0.89	0.94	0.95	0.153	0.188	0.238	0.303	0.036	0.050	0.061	0.082
100	.77	.86	.93	.95	.083	.105	.137	.179	.018	.026	.032	.043
1000	.73	.82	.89	.94	.045	.054	.075	.088	.009	.013	.017	.021
						$x(O^{++})$						
10	0.150	0.083	0.037	0.016	0.84	0.81	0.76	0.69	0.96	0.95	0.94	0.92
100	.211	.127	.057	.028	.92	.89	.86	.82	.98	.97	.97	.96
1000	.264	.176	.100	.051	.95	.95	.92	.91	.99	.99	.98	.98
						$x(Ne^+)$						
10	0.93	0.97	0.97	0.96	0.74	0.96	0.98	0.98	0.096	0.213	0.37	0.56
100	.91	.98	.98	.98	.60	.93	.97	.98	.050	.119	.23	.39
1000	.87	.99	.99	.99	.44	.87	.94	.97	.026	.064	.13	.22
						$x(Ne^{++})$						
10	0.046	0.001	0.001	0.000	0.25	0.034	0.011	0.004	0.90	0.79	0.63	0.43
100	.080	.001	.001	.000	.39	.066	.024	.009	.95	.88	.77	.61
1000	.124	.001	.001	.000	.56	.127	.054	.022	.97	.94	.87	.78
						$x(S^+)$						
10	0.38	0.40	0.42	0.48	0.090	0.106	0.126	0.165	0.024	0.033	0.036	0.047
100	.26	.27	.29	.33	.041	.049	.061	.081	.011	.014	.016	.021
1000	.16	.17	.17	.22	.020	.019	.029	.029	.004	.007	.011	.011
						$x(S^{++})$						
10	0.56	0.56	0.55	0.50	0.37	0.41	0.48	0.51	0.119	0.170	0.199	0.251
100	.65	.68	.69	.66	.25	.30	.36	.42	.059	.097	.118	.147
1000	.71	.75	.79	.76	.16	.18	.24	.27	.028	.053	.063	.076
						$x(S^{+++})$						
10	0.048	0.024	0.009	0.004	0.53	0.47	0.39	0.31	0.70	0.79	0.76	0.70
100	.086	.045	.017	.007	.70	.65	.58	.50	.66	.88	.86	.83
1000	.133	.077	.037	.016	.81	.80	.74	.70	.54	.92	.92	.91
						$x(He^+)$						
10	0.40	0.34	0.24	0.20	1.0	1.0	1.0	1.0	1.0	1.0	1.0	1.0
100	.41	.35	.24	.20	1.0	1.0	1.0	1.0	1.0	1.0	1.0	1.0
1000	.41	.35	.26	.20	1.0	1.0	1.0	1.0	1.0	1.0	1.0	1.0
						$\langle T_e \rangle_{H^+}$						
10	9880	7270	4600	1630	11600	7690	3520	720	12900	8660	4330	840
100	9980	7300	4670	1780	11700	7860	3690	860	13100	8820	4700	1100
1000	10200	7570	4910	2000	12000	8370	5020	1690	13400	9290	5710	2240
						$\langle T_e \rangle_{O^{++}}$						
10	9380	6450	2740	740	11500	7610	3430	700	12900	8680	4360	850
100	9380	6380	2613	750	11700	7810	3650	850	13100	8840	4720	1120
1000	9620	6800	3410	1000	12000	8350	4990	1680	13400	9310	5720	2260
						$\langle T_e \rangle_{N^+}$						
10	10100	7470	4900	1770	12500	8700	4710	980	13700	9880	5700	1140
100	10200	7570	5030	1950	12800	8950	5160	1230	14000	10000	6310	1560
1000	10500	7840	5260	2200	13100	9410	6410	2480	13500	10700	7030	3390

Model nebulae corresponding to each of the computed atmospheres (using the standard value of $\log g = 4$ only) were constructed for uniform hydrogen densities, n(H), of 10, 100, and 1000 cm^{-3}. Some additional models in which $\log (Z/Z_\odot) = \pm 0.5$ were also computed; for these, interpolations or extrapolations of the available atmosphere models were used. Stellar radii are taken from Panagia (1973) for luminosity class V (main-sequence) stars. The results are summarized in Tables 1 and 2.[1]

[1] Because of a computational error in the expression for the departure coefficient b_4, the Hβ fluxes used in Tables 1 and 2 should be decreased by a factor of $g = 0.2162t^{0.665} \exp\{0.9855/t\}$ for $t = \langle T_e \rangle_{H^+}/10^4 \geq 0.5$; g is given approximately by $2.28 - 3.56t + 1.87t^2$ for $0.5 \leq t \leq 1.0$.

TABLE 2B

GLOBAL OBSERVABLE PARAMETERS

T_* (K)	35,000				40,000				50,000			
log $(Z/Z_\odot)$	-0.5	0.0	0.5	1.0	-0.5	0.0	0.5	1.0	-0.5	0.0	0.5	1.0
$N(H)(cm^{-3})$						[NII]λ6583/Hβ*						
10	58	96	110	22	8.9	15.2	22.8	0.2	3.6	8.6	12.7	0.1
100	56	93	120	49	5.1	9.1	15.4	0.7	1.8	5.0	7.3	0.4
1000	55	96	120	75	3.1	5.5	8.6	5.9	0.9	2.8	5.0	4.8
						[OII]λλ3727/Hβ*						
10	250	230	92	1.0	98	99	62	<0.1	34	46	28	<0.1
100	240	220	110	6.4	57	62	44	<0.1	18	26	18	<0.1
1000	210	220	100	12.6	29	34	31	2.6	9	14	11	1.9
						[OIII]λ5007/Hβ*						
10	33	16	0.5	<0.1	350	320	200	<0.1	540	570	370	0.1
100	47	23	0.6	<0.1	390	380	230	0.6	570	610	430	1.9
1000	63	41	2.8	<0.1	440	490	340	69.	600	720	520	153
						log[NeII]λ12.8μ†						
10	-7.54	-7.09	-6.73	-6.60	-6.91	-6.40	-6.16	-6.37	-6.91	-6.17	-5.65	-5.60
100	-7.55	-7.08	-6.72	-6.58	-7.01	-6.41	-6.13	-6.26	-7.20	-6.42	-5.84	-5.62
1000	-7.56	-7.08	-6.70	-6.53	-7.15	-6.44	-6.03	-5.90	-7.47	-6.69	-6.00	-5.58
						[NeIII]λ3869/Hβ*						
10	1.7	<0.1	<0.1	<0.1	18	1.3	0.2	<0.1	110	74	24	<0.1
100	2.9	<0.1	<0.1	<0.1	31	2.8	0.4	<0.1	120	90	35	<0.1
1000	5.0	<0.1	<0.1	<0.1	49	7.4	1.0	<0.1	130	120	51	5.7
						[SII]λλ6717+6731/Hβ*						
10	43	70	86	23	16.3	29	53	0.7	6.5	14.0	23.3	0.2
100	29	48	66	43	8.3	16	34	1.9	3.1	6.7	11.5	0.7
1000	18	32	41	47	4.0	7	15	12.0	1.3	3.1	7.6	7.6
						[SIII]λ9532/Hβ*						
10	13	23	27	9	12.0	22	34	2.1	4.8	12.0	21.7	1.6
100	15	29	38	19	8.5	17	29	5.3	2.5	7.2	14.5	4.0
1000	18	35	50	36	5.5	12	24	25.8	1.2	4.3	8.5	14.6
						log[SIV]λ10.5μ†						
10	-9.14	-9.01	-9.10	-9.71	-7.35	-7.00	-6.89	-7.43	-6.36	-5.90	-5.65	-6.00
100	-8.88	-8.73	-8.82	-9.37	-7.25	-6.86	-6.68	-7.05	-6.39	-5.85	-5.56	-5.74
1000	-8.69	-8.50	-8.44	-8.84	-7.17	-6.77	-6.44	-6.43	-6.48	-5.83	-5.44	-5.33
						radio flux (Jy)†						
10	110	90	67	41	590	470	290	170	4400	3500	2400	1300
100	110	91	69	42	600	480	310	180	4500	3600	2500	1400
1000	110	93	71	44	600	490	380	230	4600	3700	2900	1800
						log(Hβ)†						
10	-7.22	-7.30	-7.76	-8.73	-6.52	-6.61	-7.20	-9.46	-5.66	-5.72	-6.17	-8.39
100	-7.22	-7.29	-7.55	-8.60	-6.52	-6.60	-7.14	-9.03	-5.66	-5.72	-6.09	-7.74
1000	-7.21	-7.28	-7.51	-8.46	-6.52	-6.59	-6.82	-7.95	-5.65	-5.70	-5.88	-6.74
						log[OIII]λ5007/λ4363						
10	2.32	2.95	4.42	>5	2.01	2.48	3.12	>5	1.87	2.30	2.98	>5
100	2.30	2.95	4.39	>5	1.97	2.42	3.03	>5	1.84	2.25	2.88	>5
1000	2.22	2.81	4.20	>5	1.88	2.32	2.82	4.31	1.77	2.15	2.75	4.05
						log[NII]λ6583/λ5755						
10	1.78	2.14	2.73	4.58	1.57	1.90	2.44	>5	1.50	1.78	2.36	>5
100	1.77	2.12	2.67	3.91	1.54	1.86	2.38	>5	1.48	1.76	2.25	>5
1000	1.76	2.05	2.61	3.62	1.51	1.82	2.22	3.51	1.50	1.69	2.16	3.23

*percent †erg cm^{-2} s^{-1} at 500 pc

The nebular average (i.e., global) structural parameters x and $\langle T_e \rangle$ shown in the tables are defined as

$$x(R^{+p}) = \frac{\int_{neb} [n(R^{+p})/n(R)] n_e d^3r}{\int_{neb} n_e d^3r} \qquad (1)$$

and

$$\langle T_e \rangle_{R^{+p}} = \frac{\int_{neb} T_e(r) n(R^{+p}) n_e d^3r}{\int_{neb} n(R^{+p}) n_e d^3r}, \qquad (2)$$

where n_e is the electron density. Various observable parameters are also shown. Line ratios relative to Hβ

are expressed as percentages. Except for the radio flux, absolute fluxes are given in cgs units and assume a distance of 500 pc to the nebula. Most entries are specified with more significance than is justified in order that trends in the data can be more readily discerned. Because ionization and thermal equilibrium are assumed throughout the nebula, the intensities of those emission lines formed preferentially at the nebular edge are probably underestimates. In addition, the accuracy of the recombination rates and recombination-line fluxes used in the program deteriorates for temperatures less than 5000 K; hence the observable parameters of the models for which $Z/Z_\odot \gtrsim 3$ become increasingly inaccurate.[2]

IV. NEW RESULTS

We shall not discuss the results of the nebular calculations in any detail, but rather we shall emphasize some of the salient results and trends.

1. Of considerable interest are the differences in the relative sizes of the zones of the different species of low (or high) ionization [compare $x(N^+)$ and $x(O^+)$; also $x(O^{++})$ and $x(Ne^{++})$]. The fractional ionization zones x are nearly independent of Z and T_e, and can be expected to pertain even if abundances or electron temperatures cannot be determined.

2. Although substantially different from unity, certain ratios of ionization-zone sizes, such as $x(N^+)/x(O^+)$, are nearly constant under a wide range of stellar temperatures and nebular densities.

3. The close coupling between Z and $\langle T_e \rangle$ is explained by the behavior of the cooling rate, as illustrated in Figure 3. The cooling rate is dominated by forbidden-line cooling from oxygen (unless the oxygen abundance is small); thus an estimate of $\langle T_e \rangle$ is a strong indication of the oxygen abundance $n(O)/n(H)$ and vice versa (see also Shields 1974).

4. The extremely small temperatures derived for nebulae of high metal abundance imply that the optical forbidden lines become less effectively excited. In this case the optical spectrum will be dominated by the recombination lines, and may also contain weak emission from forbidden lines of low excitation such as [S II] and [N II] (see spectrum of an H II region of high metal content in Smith 1975*a*, Fig. 4).

5. The rapid changes in the stellar flux near 35 eV in stars hotter than 33,000 K [which become manifest in the relative changes of the ionization-zone sizes such as $x(O^{++})/x(Ne^{++})$ with increasing T_*] makes it possible to estimate the effective color temperature of the ionizing radiation, even if the exciting stars are not directly observable. A very useful measure of the effective excitation temperature is given by the ratio of the infrared [Ne II] and [S IV] lines, provided that the relative abundances of Ne and S are known. At optical wavelengths, various ratios of the generally bright nebular lines of [O III], [Ne III], and Hβ can be used. If the density distribution can be independently determined, then the [O III]/[O II] line ratios can also be employed (see the cautionary remarks below).

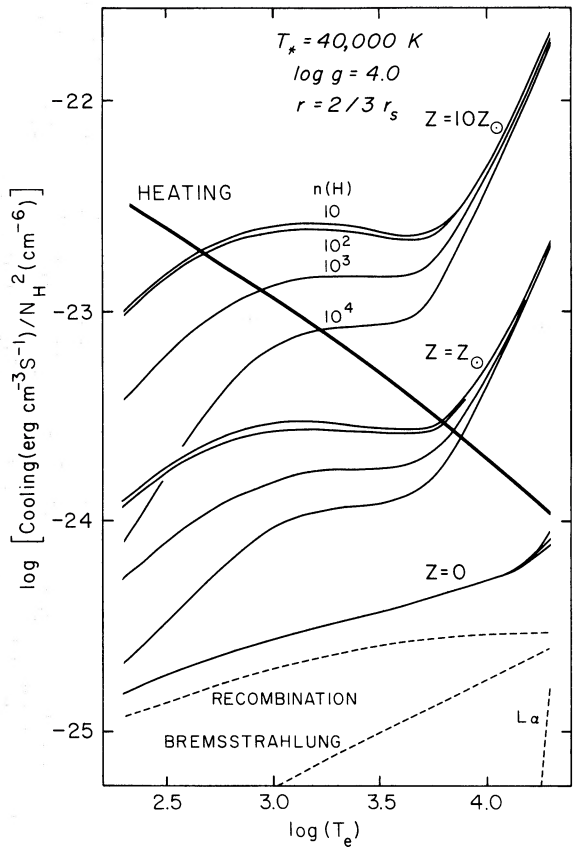

FIG. 3.—Heating and cooling rates as a function of electron temperature at a radius = 2/3 of the Strömgren radius for nebulae of various densities and metal contents. For $\log(Z/Z_\odot) \gtrsim -1$ the cooling rate is dominated by [O III] $\lambda\lambda 4959 + 5007$ emission for $T_e \gtrsim 8000$ K and by [O III] $\lambda\lambda 52\ \mu$ and $88\ \mu$ at lower temperatures. Collisional quenching of the infrared lines is important at densities $n(H) \gtrsim 500$ cm^{-3}.

V. DETERMINING METAL ABUNDANCES

As noted earlier, the determination of the metal abundances is heavily reliant on the results of model nebula calculations. Because the present model nebulae have ionization structures which differ from previous calculations, a reanalysis of the procedures used for estimating $n(Z)/n(H)$ is in order. In this section we shall investigate abundance determination schemes and the accuracy of the PTP method. Then we suggest an improved alternate method which employs semi-empirical correction factors to the PTP formulae and discuss its applicability.

[2] The referee has kindly pointed out that the neon abundance used in the present model calculations may have been overestimated by as much as an order of magnitude. Because the stellar opacity of neon is negligible at energies $\lesssim 40$ eV, and generally much less than unity at higher energies, little change in the emergent stellar spectrum or nebular ionization structure can be expected for more realistic values of $n(Ne)/n(H)$. On the other hand, the neon line intensities listed in Tables 1 and 2 should be regarded as overestimates since they are nearly proportional to the neon abundance.

Tables 1 and 2 show that the assumption of two separate ionization zones used in the PTP procedure to convert ionic species abundances into total metal abundances can result in considerable systematic errors. In order to assess the differences in the predicted abundances between the present calculations and the PTP procedure, the line intensities computed by our model nebula calculations were used as input to the PTP scheme, and the so-called PTP metal abundances were derived (mean square temperature fluctuations $t^2 = 0.055$ were assumed). The ratios of model to PTP abundances were then computed; the disparity in abundances is found to be on the order of a factor of 2 for oxygen, 3 for nitrogen, and 3–10 for neon under the conditions $Z \leqslant 2Z_\odot$, $T_* \geqslant 40{,}000$ K, and $n(\mathrm{H}) \geqslant 10^2$ cm^{-3}. These ratios increasingly differ from unity as $Z/Z_\odot$ increases or as T_* or $n(\mathrm{H})$ decreases beyond the above limits.

As noted by Peimbert (1975), some of the disagreement in the derivations of metal abundances between the original PTP scheme and more modern methods can result from the use of the revised values of atomic parameters now available. These new cross sections not only alter the coefficients of the equations of forbidden-line emissivities, but more importantly result in different estimates for $\langle T_e \rangle$ based on the [O III] or [N II] line ratios. Since the forbidden line emissivities vary approximately as $\exp(\mathrm{const}/T_e)$, the derived species abundances relative to hydrogen depend sensitively on the electron temperature, particularly for those species whose bright forbidden lines have larger excitation energies (O^{++}, Ne^{++}, and O^+).

A variation of the PTP method can be used for increased accuracy. This method, which, like the PTP procedure, is relatively insensitive to details of the density distribution compared to other methods, uses the ionization states of oxygen as a guide to the relative species abundances of the other metals. Once the best value of $\langle T_e \rangle$ is available (say, from the [O III] or [N II] line ratios and the tables), then improved ionic species abundances are obtained from the formulae of PTP as modified for new values of atomic constants.[3] The conversion from species to metal abundances is obtained as

$$\frac{n(\mathrm{O})}{n(\mathrm{H})} = \frac{n(\mathrm{O}^+)}{n(\mathrm{H}^+)} + \frac{n(\mathrm{O}^{++})}{n(\mathrm{H}^+)}, \tag{3}$$

$$\frac{n(\mathrm{N})}{n(\mathrm{H})} \approx \frac{n(\mathrm{O})}{n(\mathrm{H})} \frac{n(\mathrm{N}^+)}{n(\mathrm{O}^+)} \frac{x(\mathrm{O}^+)}{x(\mathrm{N}^+)}, \tag{4}$$

$$\frac{n(\mathrm{Ne})}{n(\mathrm{H})} \approx \frac{n(\mathrm{O})}{n(\mathrm{H})} \frac{n(\mathrm{Ne}^{++})}{n(\mathrm{O}^{++})} \frac{x(\mathrm{O}^{++})}{x(\mathrm{Ne}^{++})}, \tag{5}$$

and

$$\frac{n(\mathrm{S})}{n(\mathrm{H})} \approx \frac{n(\mathrm{O})}{n(\mathrm{H})} \frac{n(\mathrm{S}^+)}{n(\mathrm{O}^+)} \frac{x(\mathrm{O}^+)}{x(\mathrm{S}^+)}. \tag{6}$$

[3] Smith (1975*b*) has revised the PTP expressions for the ionic abundances. He finds their values of K for O^+, O^{++}, N^+, and Ne^{++} should be multiplied by factors of 0.95, 0.67, 0.74, and 0.98, respectively.

Here $n(\mathrm{N}^+)/n(\mathrm{O}^+)$, $n(\mathrm{Ne}^{++})/n(\mathrm{O}^{++})$, and $n(\mathrm{S}^+)/n(\mathrm{O}^+)$ are obtained from observed line ratios of relevant lines, and $x(\mathrm{O}^+)/n(\mathrm{N}^+)$, $x(\mathrm{O}^{++})/x(\mathrm{Ne}^{++})$, and $x(\mathrm{O}^+)/x(\mathrm{S}^+)$ are estimated from Tables 1 and 2. The ionization correction factors $x(Z_1)/x(Z_2)$ are generally fairly constant (but not generally of unit value) over a wide range of values of T_* and $n(\mathrm{H})$, as discussed in § IV. While some of the abundance disparities between the present results and the PTP scheme can be explained by differences in $\langle T_e \rangle$, for metals other than oxygen the correction factor can be quite important.

Several remarks are in order. First, both $n(\mathrm{N}^+)/n(\mathrm{O}^+)$ and $n(\mathrm{S}^+)/n(\mathrm{O}^+)$ are based on the ratios of red lines ($\lambda \approx 6500$ Å) to blue lines ($\lambda = 3727$ Å). These ratios are sensitive to both $\langle T_e \rangle$ and reddening corrections. If the [O II] lines at λ7325 Å cannot be observed, then it is common practice to replace O^+ by N^+ in equation (6) since the ratio $n(\mathrm{S}^+)/n(\mathrm{N}^+)$ can be accurately determined. Second, it should be remembered when using Tables 1 and 2B that a change in the oxygen abundance will change $\langle T_e \rangle$ and affect all forbidden-line intensities. On the other hand, small changes in the abundance of another metal will alter only the intensities of lines of that metal. Third, we emphasize that the ratio of x's given in the tables are volume averages. If the available spectra do not represent nebular averages, but rather small regions along a line of sight, then the ratios of the x's must be corrected for geometric effects, especially when the appropriate ionization zones lie in the nebular interior.

In practice it is difficult to determine metal abundances because of uncertainties in estimated values of T_e, n_e, and the rms variations of both. If extreme clumping or density concentration near the nebular edge is the case, then the method for determining abundances outlined above can give erroneous results, and full model calculations with a large number of free density parameters become necessary. Other problems have been reviewed by Miller (1974), Shields (1974), and Smith (1975*a*). Even for the most favorable nebulae, uncertainties of a factor of 2 or more would generally seem reasonable for the determination of the metal abundances unless additional lines of the ionized species, the sources of excitation, and the density distribution can be observed.

VI. ABUNDANCE GRADIENTS IN GALAXIES

Abundances and abundance gradients in other galaxies have recently been discussed by several investigators (cf. Shields 1974; Smith 1975*a*; Peimbert 1975). The existence of the Z gradient has been inferred from trends of the forbidden-line intensity ratios with galactocentric distance ρ, especially the ratios of [O III] λ5007, [O II] λ3727, [N II] λ6583, Hβ, and, where observable, the [Ne III] λ3869 and [S II] $\lambda\lambda$6717 + 6731 lines. Although the existence of the metal abundance gradients appears to be well established, the magnitude of the gradient is not well determined. Shields and Tinsley (1975) have pointed out that the magnitude of the gradient can be difficult

to estimate since a high Z abundance could conceivably alter the effective temperature of the exciting star relative to the $Z = Z_\odot$ case. However, the present calculations show that while changes in Z affect the emergent flux of the more energetic photons ($h\nu \gtrsim 35$ eV) and hence the nebular ionization structure, the total emergent fluxes and the value of T_* are not sensitive to changes in metal abundances.

Smith's (1975*a*) spectrophotometric measurements of forbidden-line intensities of H II regions show that the [O III] λ5007/[O II] λ3727 ratio varies from ~0.1 in the central parts of M101 and M33 to ~10 near the edge. The gradient of this line ratio, indicative of the nebular excitation $x(O^{++})/x(O^+)$, is accompanied by a tenfold increase in $n(O)/n(H)$. Since the Hβ fluxes from these nebulae appear to be comparable, and since the hottest stars dominate the nebular excitation, then it follows that the stellar excitation $\Phi(\lambda < 912)$ per nebula is more or less uniform (at a value consistent with $T_* \approx 40{,}000$ K), and that the depletion of 35 eV photons which decreases $x(O^{++})/x(O^+)$ is caused primarily by the increased metal content of the exciting stars at small ρ and secondarily by a gradient in T_*. The more or less constant value of the $n(He^+)/n(H^+)$ ratio is corroborative evidence that T_* always exceeds ~37,000 K. We conclude that it appears possible to explain the $x(O^{++})/x(O^+)$ gradient without a gradient in T_* so long as the Z gradient exists.

Finally, we note that little is known about a nebular metal-abundance gradient in our own Galaxy. Nebulae which span a wide range of ρ are too heavily obscured to be seen optically. Radio measurements can determine only $n(He^+)/n(H^+)$; as in other galaxies (Smith 1975*a*), no systematic trend of the ionized helium abundance as a function of ρ is seen in our galaxy. Observations of isotopic species of CO, HCN, and other molecules (Wannier *et al.* 1975) show no variations of isotopic abundances of certain metals in any of the regions studied. The innermost of the giant H II regions in our Galaxy, Sgr B2 ($\rho \lesssim 3$ kpc), appears to show radio recombination line to continuum ratios much like other giant H II regions (Chaisson 1973). The constancy of the recombination-line ratios can be taken to imply a nearly constant value for T_e and thus a nearly solar oxygen abundance throughout the Galaxy.[4] In contrast, all of the Sbc and Scd galaxies studied by Smith (1975*a*) show some evidence of metal enrichment at small values of ρ. Also, Janes and McClure (1972) have found a CN gradient with ρ in the atmospheres of galactic K giants (see also van den Bergh 1975).

VII. CONCLUDING REMARKS

We have shown that metal opacities in the atmospheres of stars which excite H II regions can have a significant effect on the predicted ionization structure of these nebulae. Generally speaking, the more energetic stellar photons are preferentially absorbed (relative to model calculations of metal-free atmospheres); hence, the predicted degree of metal ionization can drop considerably throughout the nebula, and the intensity of line emission from "low ionization" species (e.g., N^+, O^+, and Ne^+) will be somewhat larger than earlier model calculations have indicated. Moreover, the zones of "low" and "high" ionization states of He and the metals are not mutually exclusive, contrary to general assumption.

The computations presented here should be considered illustrative pending further, more accurate model atmosphere calculations. For example, the effects of spherical symmetry and ultraviolet line blanketing on the emergent flux require further investigation. It is clear, however, that the "depletion" of energetic stellar photons, often attributed to the presence of nebular dust with a sharply increasing cross section at energies above the Lyman limit (cf. Mezger, Smith, and Churchwell 1974), may result instead from various processes in the stellar atmosphere. Further observations of the distribution of infrared emission in H II regions (see, e.g., Gehrz, Hackwell, and Smith 1975) will be of interest in this regard.

It is a pleasure to thank H. E. Smith, R. L. Kurucz, and D. Carbon for interesting discussions and advice. Ms. Judy Bell and Ms. Laura Toepfer prepared the manuscript and figures. Financial support was provided by NSF grant 73-08981 A02 and Lick Observatory.

[4] Lockman and Brown (1975) have shown that a rather specific knowledge of the nebular density and geometry are required before T_e can be derived from radio recombination lines. Thus it is possible that a systematic trend of the density distribution with ρ can obviate the effects of a T_e gradient in these radio measurements. In this regard, it should be noted that Sgr B2 is the densest and most massive of the galactic H II regions (Balick and Sanders 1974; Chaisson 1973).

REFERENCES

Auer, L. H., and Mihalas, D. 1972, *Ap. J. Suppl.*, **24**, 193.
Balick, B. 1975, *Ap. J.*, **201**, 705.
Balick, B., and Sanders, R. H. 1974, *Ap. J.*, **191**, 325.
Boeshaar, G. O. 1975, *Ap. J.*, **195**, 695.
Casinelli, J. P. 1971, *Ap. J.*, **165**, 265.
Casinelli, J. P., and Hartmann, L. 1975, preprint, Univ. Wisconsin Ap. Series No. 14.
Chaisson, E. J. 1973, *Ap. J.*, **186**, 555.
Gehrz, R. D., Hackwell, J. A., and Smith, J. R. 1975, *Ap. J. (Letters)*, **202**, L33.
Hjellming, R. M. 1966, *Ap. J.*, **143**, 420.
Hummer, D. G., and Mihalas, D. 1970*a*, *Joint Inst. for Lab. Ap. Reports*, No. 101.
Hummer, D. G., and Mihalas, D. 1970*b*, *M.N.R.A.S.*, **147**, 339.
Janes, K. A., and McClure, R. D. 1972, in *l'Age des Etoiles, IAU Colloquium No. 17*, ed. G. Cayrel de Strobel and A. M. Delplace (Meudon: Observatoire de Paris), p. xxviii.
Kurucz, R. L. 1970, *Smithsonian Ap. Obs. Spec. Rept.*, No. 309.
Lockman, F. J., and Brown, R. L. 1975, preprint.
Mezger, P. G., Smith, L. F., and Churchwell, E. 1974, *Astr. and Ap.*, **32**, 269.
Miller, J. S. 1974, *Ann. Rev. Astr. and Ap.*, **12**, 331.
Osterbrock, D. E. 1970, *Quart. J.R.A.S.*, **11**, 199.
———. 1974, *Astrophysics of Gaseous Nebulae* (San Francisco: W. H. Freeman).

Panagia, N. 1973, *A.J.*, **78**, 929.
Peimbert, M. 1975, *Ann. Rev. Astr. and Ap.*, **13**, 113.
Peimbert, M., and Costero, R. 1969, *Bol. Obs. Tonantzintla y Tacubaya*, **5**, 3.
Peimbert, M., and Torres-Peimbert, S. 1971, *Ap. J.*, **168**, 413.
Rubin, R. H. 1969, *Ap. J.*, **155**, 841.
Searle, L. 1971, *Ap. J.*, **168**, 327.
Seaton, M. J. 1975, *M.N.R.A.S.*, **170**, 475.
Shields, G. A. 1974, *Ap. J.*, **193**, 335.
Shields, G. A., and Tinsley, B. M. 1975, preprint, Univ. of Texas at Austin.
Smith, H. E. 1975*a*, *Ap. J.*, **199**, 591.
———. 1975*b*, private communication.
Terzian, Y., and Balick, B. 1974, *Fund. Cosmic Phys.*, **1**, 301.
van den Bergh, S. 1975, *Ann. Rev. Astr. and Ap.*, **13**, 217.
Wannier, P. G., Penzias, A. A., Linke, R. A., and Wilson, R. W. 1975, preprint, Bell Laboratories Technical Memorandum.

BRUCE BALICK: Astronomy Department, University of Washington, Seattle, WN 98195

CHRISTOPHER SNEDEN: Department of Physics and Astronomy, University of Wyoming, University Station, Box 3905, Laramie, WY 82071